Coupling phenomena and vortex transitions in superconducting Ni/Nb multilayers

E. C. Siqueira · O. F. de Lima

Abstract We have studied some structural and superconducting properties of Ni/Nb multilayered films prepared by magnetron sputtering. Magnetization measurements allowed us to establish a rich $H \times T$ diagram that indicates a 3D-2D dimensional crossover of the vortex system, as revealed by the parallel upper critical field behavior. Consistently, it was identified a possible decoupling line associated with the transition of Abrikosov vortex lines into vortex pancakes, starting around the same crossover region. An irreversibility line was also determined and it suggests different regimes of the vortex matter, where the role played by the Ni ferromagnetic layers might be relevant.

Introduction

Superconductor/ferromagnetic (S/F) multilayers have been intensively studied because of the interesting proximity effects close to the interfaces [1, 2], as well as due to the prospects for applications in nanotechnology. A great survey of experimental data have been reported, discussing the superconducting critical temperature (T_c) dependence on the layers thicknesses [2, 3]. Earlier studies in Ni/Nb multilayers have investigated essentially the variation of T_c as a function of the Ni and Nb layer thicknesses, respectively t_{Ni} and t_{Nb}. [3–9]. For bilayer systems it has been observed that T_c

oscillates as function of t_{Ni} [6]. These oscillations were explained by a proximity effect theory applied to the S/F layers [10]. Other studies have reported a monotonic decrease of T_c with the increase of t_{Ni}. However all works agree that T_c decreases by decreasing t_{Nb}, as well as that superconductivity is suppressed when $t_{Nb} < 100$ Å and $t_{Ni} > 20$ Å. A search for interlayer magnetic coupling, mediated by superconducting Nb layers, has been attempted [4]. However, the proximity effect between Nb and Ni was found to suppress superconductivity strongly for thin Nb layers, thus precluding the hypothesized coupling.

Measurements of the perpendicular and parallel upper critical fields (H_{c2}) give important information about dimensionality of the superconducting phase in multilayered systems [11]. As far as we know the reported results on the Ni/Nb system have not identified yet any dimensional crossover of the superconducting phase. This could be investigated, for instance, by measuring the upper critical field parallel to the layers as a function of temperature, $H_{c2}^{ab}(T)$, which is expected to show a parabolic behavior in the bi-dimensional (2D) case and a linear behavior in the three dimensional (3D) case [11]. In S/F multilayered systems, the dimensional crossover (3D-2D) of superconductivity has been reported only for V/Fe, Nb/Fe and Nb/Co [12–14], thus requiring more studies in this area. In the high-T_c superconductors $Bi_2Sr_{2-x}La_{x-}CuO_{6+\delta}$ and $Bi_2Sr_2CaCu_2O_{8+\delta}$, a different dimensional transition was observed which is characterized by a double transition in the magnetization curves ($M \times T$) [15, 16]. One explanation of this unusual behavior was made [17] by considering that the first transition at higher T is produced by the individual superconducting grains, and the second transition at a lower T is due to

E. C. Siqueira · O. F. de Lima (✉)
Instituto de Física Gleb Wataghin, UNICAMP, Campinas 13083-970, SP, Brazil
e-mail: delima@ifi.unicamp.br

a Josephson coupling between those grains. This type of coupling mechanism has not been observed in artificially-grown multilayered systems yet. Another possible explanation for the observed transition at lower T could be the vortex decoupling, going from a 3D Abrikosov lattice to a 2D pancake lattice [18]. This would occur when the coherence length becomes smaller than the Nb layer thickness, therefore confining superconductivity within each Nb layer.

In this work, a dimensional crossover of superconductivity is reported for a S/F multilayered sample of Ni/Nb. This result was obtained from magnetization curves that were measured under magnetic fields applied in parallel and perpendicular directions relative to the layers. The upper critical field line perpendicular to the layers $(H^c_{c2}(T))$ shows a slight upward deviation which is oftenly observed in granular as well as in layered systems [14, 19]. The irreversibility line was also obtained, thus producing a rich $H \times T$ diagram possibly related to different phases of the vortex matter in this system.

Materials and methods

The Ni/Nb multilayers were grown by magnetron sputtering on a 90° sapphire substrate kept at room temperature and in an Ar (99.999% purity) atmosphere of 3 mTorr. Pure Nb(99.99%) and Ni (99.9%) elements were used as sputtering targets with deposition rates in the range of 3–4 Å/s and a substrate-to-target distance of 9 cm. The base pressure of the sputtering system was 1×10^{-7} Torr. All samples were made having Ni layers in both outer surfaces. Two types of Nb/Ni multilayer structures were prepared. One having a fixed Nb layer thickness $d_{Nb} = 90$ Å and a varying Ni thickness from $d_{Ni}=0–24$ Å, with 19 bilayers in each sample, where d_{Nb} and d_{Ni} represent nominal values. The other type was made having a fixed $d_{Ni} = 20$ Å and a varying d_{Nb} from 0 to 250 Å, with 9 bilayers in each sample.

Small angle X-ray diffraction (XRD) scans ($2\theta < 4°$, CuKα radiation) were used to determine the bilayer thicknesses of the samples. Figure 1 shows a typical XRD pattern measured for sample Ni/Nb-A with nominal composition Ni(20 Å)[Nb(250 Å)/ Ni(20 Å)]$_9$. In general a multilayer pattern presents two superimposed oscillations, the first having a shorter period is related with constructive and destructive X-ray interferences at the surfaces and interfaces of the layers. The second, having a longer oscillation period, is related to the double layer thickness or modulation wavelength $\Lambda = t_{Ni} + t_{Nb}$. The position, form and
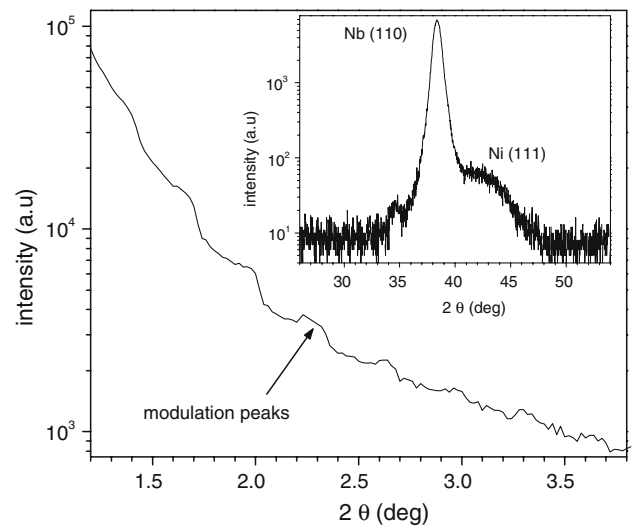
Fig. 1 Small and high angle (inset) X-ray diffraction patterns for a multilayer sample with actual composition Ni(18.7 Å) [Nb(232.5 Å)/ Ni(18.7 Å)]$_9$

intensity of the interference maxima are strongly influenced by the roughness of the surface and interfaces. As shown in Fig. 1 the peaks with short period are almost completely suppressed in the XRD pattern measured in our sample, possibly indicating the occurrence of rough interfaces caused by mutual interdiffusion of Ni and Nb atoms. However, the bilayer peaks are well defined, which reveals a good composition modulation of the probed sample. Its modulation length, $\Lambda = 251.2$ Å, was obtained from the angular position of the bilayer peaks (Fig. 1). Similar bilayer patterns were obtained for a total of seven samples ($d_{Nb} = 250, 200, 150, 120, 90, 60$ and 20 Å) with a fixed Ni thickness of nominal value $d_{Ni} =20$ Å. The solid line in Fig. 2 represents a linear fit to the $\Lambda \times d_{Nb}$ plot, whose ordinate at $d_{Nb} = 0$ gives the actual Ni layer averaged thickness of 18.7 Å. Its angular coefficient works as a correction factor that multiplied by d_{Nb} gives the actual Nb layer thickness.

Therefore the actual composition of sample Ni/Nb-A was found to be Ni(18.7 Å)[Nb(232.5 Å)/ Ni(18.7 Å)]$_9$. The inset of Fig. 1 shows the high-angle diffraction pattern for sample Ni/Nb-A. The peaks obtained in this high-angle region are associated with scattering from individual Nb and Ni layers with (110) and (111) textures, respectively. In the rest of this paper some remarkable superconducting properties of sample Ni/Nb-A, mainly related to a dimensional crossover of the vortex system, will be discussed. Those properties were measured with a Superconducting Quantum Interference Device (SQUID), model MPMS-5, made by Quantum Design Co.
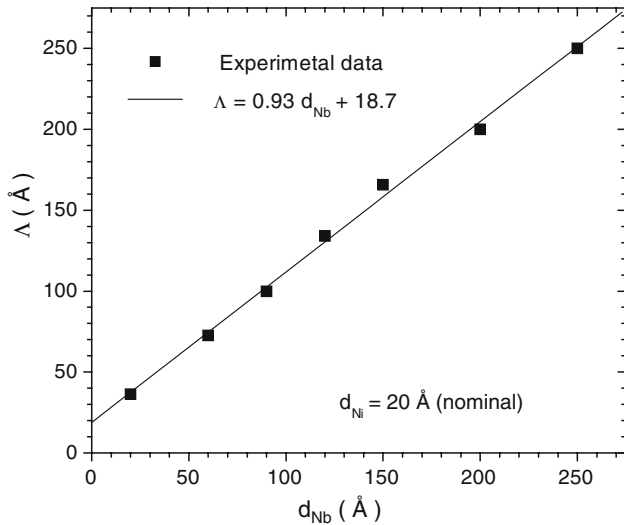
Fig. 2 Multilayer modulation length as a function of the nominal Nb thickness. The angular coefficient of the fitted straight line is a factor that multiplied by d_{Nb} gives the actual Nb thickness and the ordinate at $d_{Nb} = 0$ gives the actual Ni layer thickness

Results and discussion

Figure 3 shows the magnetic moment (M) of sample Ni/Nb-A measured as a function of temperature for several applied fields perpendicular to the layers. Zero Field Cooling (ZFC) and Field Cooling measured on Cooling (FCC) processes were employed, although only the ZFC measurements are shown here for clarity. For the higher fields one sees a monotonic increase of
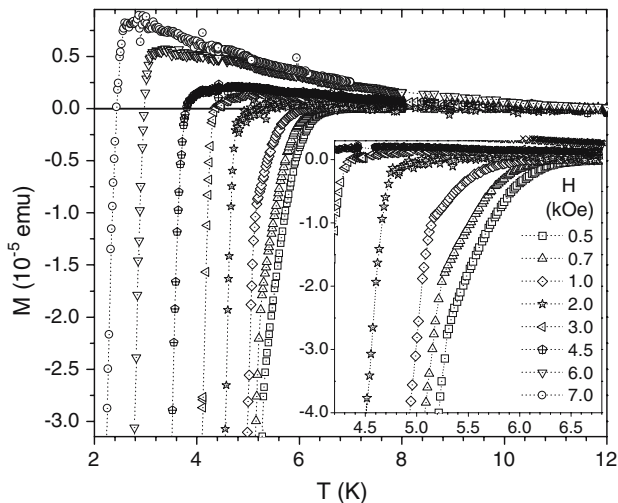
Fig. 3 Magnetic moment as a function of temperature (ZFC) for a Ni(18.7 Å)[Nb(232.5 Å)/Ni(18.7 Å)]₉ multilayer under several applied fields. The inset is an enlarged view that evidences a clear knee in some of the $M \times T$ curves, attributed to a vortex decoupling transition

M when T decreases, attributed to the ferromagnetic response from the Ni layers. The temperature at the onset of transition corresponds to the bulk nucleation of superconductivity, associated with the upper critical field. A vortex decoupling temperature, T_{dec}, was defined at the point where the $M \times T$ curve changes its slope, producing a clear knee for fields between 0.5 and 3.0 kOe as shown in the inset of Fig. 3.

Figure 4 presents some characteristic $H \times T$ lines, extracted from the measured $M \times T$ curves for H perpendicular and parallel (not shown here) to the multilayers. The filled triangles and the crossed circles represent the upper critical fields, parallel (H_{c2}^{ab}) and perpendicular (H_{c2}^{c}), respectively. For temperatures above 5.8 K both H_{c2} lines show an almost linear behavior, as expected for a 3D nucleation field [20]. Around $T^* = 5.42$ K H_{c2}^{ab} changes dramatically, going up very rapidly for $T < T^*$. This anomaly is interpreted to be a signature of dimensional crossover, fitted here (dashed line in Fig. 4) by $H_{2D}(T) = 27.8 \left(1 - T/5.38\right)^{1/2}$, which follows exactly the temperature dependence predicted for a 2D behavior [11]. A reasonable interpretation for the crossover region of H_{c2}^{ab} around T^* was possible by using the following expression [11] based on the Lawrence-Doniach (LD) [21] theory for Josephson coupled layers:
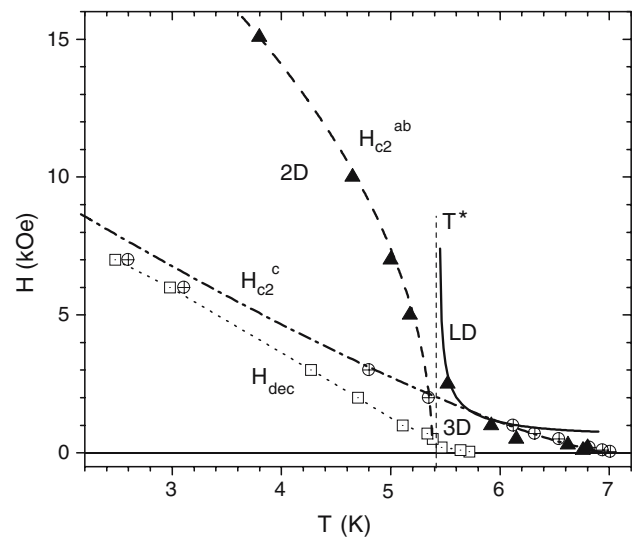
Fig. 4 Some characteristic lines that were extracted from the measured $M \times T$ curves for sample Ni(18.7 Å)[Nb(232.5 Å)/Ni(18.7 Å)]₉. The filled triangles and the crossed circles represent, respectively, the upper critical fields parallel (H_{c2}^{ab}) and perpendicular (H_{c2}^{c}) to the layers. The open squares represent the vortex decoupling line. The line LD represents a fit of the Lawrence–Doniach theory and $T^* \approx 5.42$ K is the crossover temperature where the vortex system undergoes a dimensional transition. The other fitted lines are explained in the text

$$H_{c2}^{ab}(T) \approx \frac{\xi^{ab}(T)\,\xi^c(T)\,H_{c2}^c(T)}{\Lambda^2\left[1 - \Lambda^2/2\,(\xi^c(T))^2\right]^{1/2}}\cdot, \quad (1)$$

where [20] $\xi^{ab}(T) = \xi_0^{ab}(1 - T/T_c)^{-\nu}$ and $\xi^c(T) = \xi_0^c(1 - T/T_c)^{-\nu}$ are the parallel and perpendicular coherence lengths, respectively, and $H_{c2}^c(T) = \Phi_0/2\pi(\xi^c(T))^2$. The critical exponent ν can be equal to 1/2 (mean field regime) or 2/3 (fluctuation regime near T_c) [22], and $\Phi_0 = 2.07 \times 10^{-7}$ Gcm^2 is the flux quantum. Using these definitions and the anisotropy parameter $\Gamma = \xi_0^{ab}/\xi_0^c$, Eq. (1) can be rewritten as:

$$H_{c2}^{ab}(T) \approx \frac{\Phi_0}{2\pi\Gamma\Lambda^2\left[1 - \Lambda^2(1 - T/T_c)^{2\nu}/2\,(\xi_0^c)^2\right]^{1/2}}\cdot \quad (2)$$

The solid line marked as LD in Fig.4 is a plot of Eq. 2 with $\xi_0^c = 62$ Å, $\Gamma = 6.6$, $\nu = 2/3$, $T_c = 6.9$ K and $\Lambda = 250$ Å. The latter two values are within 1% of the experimentally determined values for T_c and Λ, and the relatively high anisotropy parameter implies an in-plane coherence length $\xi_0^{ab} = 409$ Å, which is a typical value for very pure Nb bulk samples [23]. We have verified that the exponent $\nu = 2/3$ produces a better fit than $\nu = 1/2$, meaning that thermal fluctuations are playing an important role for $T > T^*$ in the very thin multilayers. Consistently, the perpendicular upper critical field data was well fitted by $H_{c2}^c(T) = 14(1 - T/T_c)^{2\nu}$, with $\nu = 2/3$ and $T_c = 7$ K, for $T > T^*$. Therefore, an upward curvature of $H_{c2}^c(T)$ is observed approaching T_c, instead of the expected straight line behavior. Other explanations, connected with granular or layered superconductors, have also been suggested [14, 19] to account for observed upward curvatures in the upper critical field.

It has been proposed that the anomalous increase of $H_{c2}^{ab}(T)$ around T^* happens when $\xi^c(T)$ decreases below a size that allows the vortex cores to fit between the Nb layers, hence depressing the pair braking mechanism due to electronic orbital effects [11]. This special situation corresponds to $\xi^c(T^*) = \Lambda/\sqrt{2}$ and makes Eq. 1 go asymptotically to infinity when approaching $T^* = 5.42$ K. This means that for $T < T^*$ the perpendicular coherence length becomes smaller than Λ, thus suppressing the coupling between the layers and establishing a 2D regime. However, even for $T < T^*$ the $H_{c2}^c(T)$ line still retains its almost linear T dependence expected for a 3D regime, since there are no geometrical restrictions upon $\xi^{ab}(T)$. In the case of sample Ni/Nb-A, where $\Lambda \approx 251$ Å from the X-ray analysis, one gets $\xi^c(T^*) = \Lambda/\sqrt{2} \approx 177$ Å, in good

agreement with the value calculated by $\xi^c(T^*) = 62(1–5.42/6.9)^{-2/3} \approx 174$ Å. This result corroborates strongly the hypothesis of dimensional crossover as discussed above.

The open squares in Fig. 4 represent the decoupling line, $H_{\mathrm{dec}}(T)$, associated with the decoupling temperatures, $T_{\mathrm{dec}}(H)$. This $H_{\mathrm{dec}}(T)$ line is quite different from what has been observed in the highly anisotropic high-T_c crystals [24], especially in Bi-2212 [15, 16]. Much possibly this is a consequence of the different underlying physics involved in the Ni/Nb multilayers, where it is imperative to take into consideration the role played by the ferromagnetic Ni layers and their induced proximity effects [1]. By now we have no conclusive interpretation about the $H_{\mathrm{dec}}(T)$ data, so the experimental points in Figs. 4 and 5 are connected by a dotted line only to provide a guide to the eyes. However it is noteworthy that this line starts effectively around T^* and gradually approaches the $H_{c2}^c(T)$ data (crossed circles) going to lower temperatures, as shown in a detailed view of Fig. 5. This figure displays also the irreversibility line (filled circles), $H_{\mathrm{ir}}(T) = 15.9\,(1 - T/7)^{2.1}$, which was fitted to the irreversibility points defined at the departure temperature between the ZFC and FCC measurements. Here it should be noted the occurrence of an interesting crossing point between the $H_{\mathrm{ir}}(T)$ and $H_{\mathrm{dec}}(T)$ lines near T^*, for $H \approx 700$ Oe (see inset of Fig. 5). This could indicate that the irreversibility line might be associated with a depin-
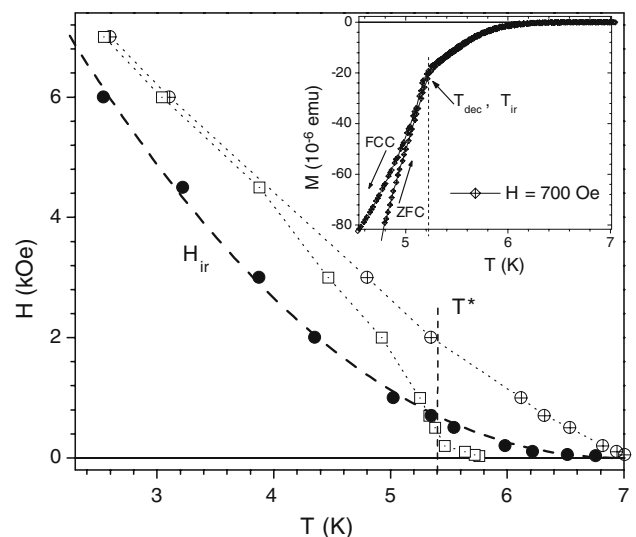
Fig. 5 The crossed circles, open squares and closed circles represent the $H_{c2}^c(T)$, $H_{\mathrm{dec}}(T)$, and $H_{\mathrm{ir}}(T)$ lines, respectively, for sample Ni(18.7 Å)[Nb(232.5 Å)/ Ni(18.7 Å)]$_9$. The inset illustrates the criterion used to identify the irreversibility points in the $M \times T$ curves, at the departure temperature between the ZFC and FCC measurements

ning or melting transition [24] of a system of 3D vortex lines for $T > T^*$, or a system of 2D vortex pancakes confined in the Nb layers for $T < T^*$. More work are on the way in sample Ni/Nb-A as well as in other multilayered samples, aimed at a more complete explanation of their rich H T diagram, and the results will be published elsewhere.

Conclusions

Ni/Nb multilayered films were prepared by magnetron sputtering and their actual layer thicknesses were determined by small angle X-ray diffraction. Magnetization curves as a function of temperature (for several applied magnetic fields) and as a function of field (for several fixed temperatures) were measured in a sample with composition Ni(18.7 Å)[Nb(232.5 Å)/ Ni(18.7 Å)]$_9$. The upper critical field lines parallel, $H_{c2}^{ab}(T)$, and perpendicular, $H_{c2}^{c}(T)$, to the layers and a decoupling line, $H_{dec}(T)$, provide consistent signatures for a 3D-2D dimensional crossover of the vortex system. Below the crossover temperature, $T^* = 5.42$ K, a 2D regime is well described by $H_{c2}^{ab}(T) \propto (1 - T/5.38)^{1/2}$, while for $T > T^*$ a 3D regime follows an almost linear dependence. An irreversibility line, $H_{ir}(T) \propto (1-T/7)^{2.1}$, was also established and seems to be associated with a depinning or melting transition of the system of 3D vortex lines for $T > T^*$, or the system of 2D vortex pancakes for $T < T^*$.

References

1. Buzdin AI (2005) Rev Mod Phys 77:935
2. Jin BY, Ketterson JB (1989) Adv Phys 38:189
3. Izyumov AY, Proshin YN, Khusainov MG (2002) Physics-Uspekhi 45:109
4. Mattson JE, Osgood RM III, Potter CD, Sowers CH, Bader SD (1997) J Vac Sci Technol A 15:1774
5. Pérez-Frias MT, Vicent JL (1988) Phys Rev B 38:9503
6. Sidorenko AS, Zdravkov VI, Prepelitsa AA, Helbig C, Luo Y, Gsell S, Schreck M, Klimm S, Horn S, Tagirov LR, Tidecks R (2003) Ann Phys (Liepzig) 12:37
7. Kryukov SA et al (2003) Ieee Trans Mag 39:2693
8. Navarro E, Villegas JE, Vicent JL (2002) J Magn Magn Mater 240:586
9. Villegas JE, Navarro E, Jaque D, González EM, Martín JI, Vicent JL (2002) Physica C 369:213
10. Radovíc Z, Dobrosavljevic L, Clem JR (1988) Phys Rev B 38:2388
11. Klemm RA, Luther A, Beasley MR (1975) Phys Rev B 12:877
12. Koorevaar P, Suzuki Y, Coehoorn R, Aarts J (1994) Phys Rev B 49:441
13. Verbank G, Potter CD, Metlushko V, Schad R, Moshchalkov VV, Bryunseraede Y (1998) Phys Rev B 57:6029
14. Obi Y, Ikebe M, Wakou H, Fujimori H (1999) J Phys Soc Jpn 68:2750
15. Wen HH, Yang WL, Zhao ZX, Ni YM (1999) Phys Rev Lett 82:410
16. de Lima OF, Awana VPS, Ribeiro VPS, Avila MA (2000) Europhys Lett 51:174
17. Geshkenbein VB, Ioffe LB, Millis AJ (1998) Phys Rev Lett 80:5778
18. Glazmann LI, Koshelev AE (1991) Phys Rev B 43:2835
19. Ikebe M, Fujishiro H, Obi Y, Fujimori H, Morohashi S (1998) Physica C 317:142
20. Tinkham M (1996) Introduction to superconductivity. McGraw-Hill, NY, p 84
21. Lawrence WE, Doniach S (1971) In: Proceedings of the 12th Int. Conf. on Low Temp. Physics. Kyoto, Japan, 1970 (Keigaku, Tokyo)
22. Bulaevskii LN, Ginzburg VL, Sobyanin AA (1988) Sov Phys Jetp 68:1499
23. Finnemore DK, Stromberg TF, Swenson CA (1966) Phys Rev 149:231
24. Blatter G, Feigel'man MV, Geshkenbein VB, Larkin AI, Vinokur VM (1994) Rev Mod Phys 66:1125